ELSEVIER

SCIENCE DIRECT®

Journal of Geodynamics 38 (2004) 131–145

JOURNAL OF GEODYNAMICS

http://www.elsevier.com/locate/jog

Tectonic displacement and far-field isostatic flexure of pluvial lake shorelines, Dixie Valley, Nevada

S. John Caskey[a,*], Alan R. Ramelli[b]

[a] *Department of Geosciences, San Francisco State University, San Francisco, CA 94132, USA*
[b] *Nevada Bureau of Mines and Geology, University of Nevada, Reno, NV 89557, USA*

Received 4 November 2003; received in revised form 10 June 2004; accepted 24 June 2004

Abstract

Shoreline features formed by the late Pleistocene pluvial Lake Dixie in Dixie Valley, central Nevada, record crustal deformation resulting from isostatic rebound of the Lake Lahontan basin, and from Holocene and historic surface faulting. Constructional beach bars on the east side of Dixie Valley show eastward tilt of 0.16 m/km, indicating that lithospheric flexure due to isostatic rebound is symmetrical with the west side of the Lahontan basin. The tilt signal is potentially complicated by post-Lake Dixie fault displacements on the west side of the valley. However, elevation changes recorded geodetically across the analogous 1983 Borah Peak, Idaho earthquake ruptures suggest that coseismic deformation is probably not significant on the east side of the valley relative to the shoreline elevation uncertainties and the overall tilt signal. A survey of faulted shorelines on the west side of the valley suggest that previous fault slip rates estimated from an earlier survey of these same shorelines are in error by nearly a factor of two. Better constrained slip rates from elsewhere along the fault indicate Holocene vertical slip rates of 0.3–0.5 mm/a, consistent with estimates of long term slip rates on the Dixie Valley fault.

1. Introduction

Pluvial lakes occupied most of the topographically closed valleys of the Great Basin during periods of the late Pleistocene when climatic conditions were cooler and/or wetter than today. The two largest of these paleolakes, Lake Bonneville and Lake Lahontan, formed on opposite sides of the Great Basin. These

* Corresponding author. Tel.: +1 415 405 0353; fax: +1 415 338-7705.
E-mail address: caskey@sfsu.edu (S.J. Caskey).

0264-3707/$ – see front matter
doi:10.1016/j.jog.2004.06.001

two lakes integrated multiple valleys and covered areas greater than 51,600 and 21,800 km^2, respectively (Mifflin and Wheat, 1979).

Gilbert (1890) first recognized that originally horizontal paleoshorelines formed during the Lake Bonneville highstand were warped upward by as much as 50 m due to isostatic rebound of the desiccated lake basin. Crittenden (1963) and Currey (1982) later showed the amount of post-Lake Bonneville rebound to be greater than 60 m. Similar studies in the smaller Lake Lahontan basin (Mifflin and Wheat, 1971; Adams et al., 1999) show more than 20 m of isostatic rebound. Data from these and other shoreline surveys have been used to not only characterize the deformation in the basins, but also to model lithospheric thickness and effective upper-mantle viscosity in the two regions (Brotchie and Silvester, 1969; Walcott, 1970; Passey, 1981; Nakiboglu and Lambeck, 1982; Bills and May, 1987; Bills et al., 1995; Adams et al., 1999).

May et al. (1991) used shoreline elevations from three valleys west of the Lake Bonneville basin to provide an extended lithospheric deflection datum. They found shorelines in these three valleys to be tilted progressively less (0.23–0.11 m/km) away from the center of maximum Lake Bonneville uplift. These data support the lithospheric thickness and upper-mantle viscosity constraints of Bills and May (1987). There have been no similar detailed studies of paleoshoreline deflections in the neighboring valleys outside the Lake Lahontan basin.

Dixie Valley is separated from the Lake Lahontan basin by the Stillwater Range (Fig. 1) and is one of the topographically lowest valleys in the northern Great Basin. The valley was occupied by the latest Pleistocene pluvial Lake Dixie, which was not connected to Lake Lahontan. Lake Dixie, at its highstand elevation of ∼1097 m, had a surface area of 715 km^2 and a maximum water depth of ∼70 m (Mifflin and Wheat, 1979). The highstand shorelines of Lake Dixie have been radiocarbon dated from tufa at 12–13 ka (Thompson and Burke, 1973; J. Bell, Nevada Bureau of Mines and Geology, unpublished data), indicating that the Lake Dixie highstand was approximately coeval with the Lake Lahontan highstand to the west, which has been dated at ∼13 ka (Broecker and Kaufman, 1965; Benson and Thompson, 1987; Adams and Wesnousky, 1998).

Pluvial Lake Dixie is ideally located for the purpose of extending the isostatic deflection signal of the Lake Lahontan basin because of its close proximity to the region of maximum rebound in the Carson Sink (Fig. 1). However, the paleoshorelines of Lake Dixie have received only reconnaissance study (Thompson and Burke, 1973; Mifflin and Wheat, 1979). Thompson and Burke (1973) mapped and locally surveyed highstand shorelines along the west side of the valley where they are offset by Holocene normal-fault ruptures along the Stillwater (seismic) gap segment of the Dixie Valley fault (Fig. 2). An extension rate of 1 mm/a across Dixie Valley based on their study is often cited in the literature. A resurvey of the shorelines in the same area using modern surveying techniques, together with recent mapping along the fault trace, shows that Thompson and Burke's (1973) surveyed elevations of the offset shorelines are in error by about a factor of two. Therefore, the extension rate based on their study needs to be reevaluated.

This paper presents results of recent shoreline elevation surveys in Dixie Valley. We first report the results of a total-station survey of the faulted shorelines previously surveyed by Thompson and Burke (1973). We then present elevation measurements of Lake Dixie highstand shorelines from around the valley to document far-field, lithospheric flexure related to isostatic rebound of the Lake Lahontan basin. Recent faulting related to regional Basin and Range extension has deformed shorelines along the west side of the valley, so we speculate on the relative influences of tectonics and isostatic flexure on the shoreline deflection signal.

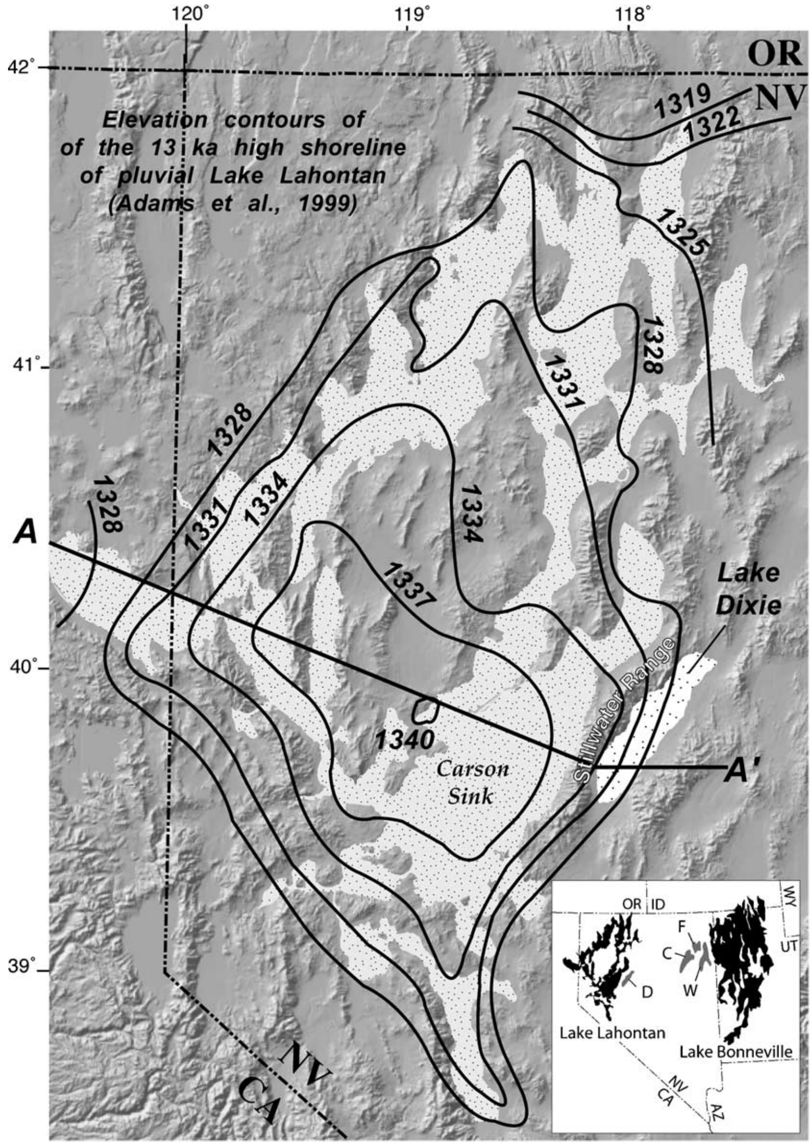

Fig. 1. Elevation contours of the 13 ka high shoreline of pluvial Lake Lahontan based on 170 high shoreline measurements (adapted from Adams et al., 1999). The contour interval is 3 m. The elevation data show the now desiccated Lake Lahontan basin has isostatically rebounded more that 20 m. Inferred projections of the elevation contours outside the Lahontan basin suggest that 6 or more meters of rebound might be expected across Dixie Valley. A–A′ marks the position of the lithospheric deflection profile shown in Fig. 8. Inset map shows the locations of pluvial lakes Lahontan, Bonneville, Dixie (D), and three pluvial lake basins in eastern Nevada; Waring (W), Clover (C), and Franklin (F), studied by May et al. (1991) to extend the lithospheric deflection datum of the Bonneville basin. Base map and lake outlines are from Reheis (1999).

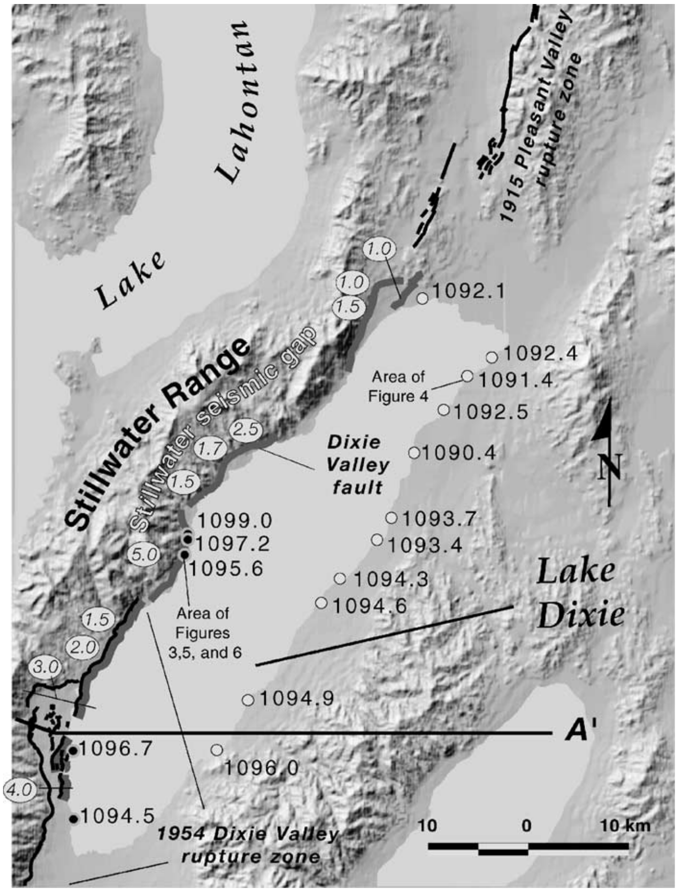

Fig. 2. High-level shoreline elevations for the ∼12 ka Lake Dixie shorelines. Elevations on the east and north shore (white circles) are from beach bar crests. Those on the west shore (black circles) represent the highest identified shorelines locally, and consist variably of cemented beach rock ledges, shoreline angles of wave-cut terraces, and high-shoreline gravel. Generalized Holocene fault rupture zones are shown as thick gray fault lines. Historic fault ruptures are shown as thin black lines. The Stillwater seismic gap represents a 46 km segment of the Dixie Valley fault between the historic 1915 Pleasant Valley and 1954 Dixie Valley earthquake ruptures to the north and south, respectively. This segment has not ruptured historically. Representative net vertical offsets measured across the zone of Holocene and historic fault scarps are shown west of the Dixie Valley fault (ovals) and are given in meters (Caskey et al., 1996; Caskey, in preparation). Black line A′ is the eastern end of the lithospheric deflection profile line shown in Fig. 1 and profile shown in Fig. 8. The Lake Dixie shoreline elevations on Fig. 7 are projected orthogonally onto the east–west part of the profile line. Areas of Figs. 3–6 are shown. Base map and lake outlines from Reheis (1999).

2. Methods and shoreline elevation uncertainties

Paleoshoreline elevations were surveyed using both total station (theodolite and electronic distance measurer (EDM)) and Global Positioning System (GPS) techniques. Along the west side of the valley, we surveyed shoreline elevations relative to National Geodetic Survey benchmarks established along S.R.

121 (Dixie Valley Road). We used benchmark elevations adjusted to the 1988 North American vertical datum (NAVD 88). The total station used has a precision of ±2 s, which equates to elevation precision of about ±3 cm across our maximum shot distances of <3 km.

On the east side of the valley, where there are no benchmarks, we surveyed shoreline elevations using a differential GPS array tied to a benchmark on the west side of the valley. We employed Trimble 4000Ssi GPS receivers with choke-ring antennas that enabled us to achieve centimeter-level vertical and horizontal accuracy. The largest source of uncertainty in the GPS measurements comes from the estimated geoid separation (i.e., difference between GPS height and elevation above mean sea level), which is on the order of a few decimeters.

Lake Dixie highstand shorelines are only locally preserved along the west side of the valley, mainly along the steep frontal escarpment of the Stillwater Range (i.e., the footwall of the Dixie Valley normal fault). There, shoreline features consist primarily of wave-cut strandlines and cemented beach-rock ledges (Fig. 3). These features approximate the highstand elevation, but the lake may have risen higher than these levels without leaving an "indelible" record of the highstand. In the Lake Lahontan basin, Adams et al. (1999) found that high-level shoreline angles of wave-cut terraces are consistently 1–3 m lower than the crests of adjacent constructional (i.e., depositional) beach ridges. Therefore, we consider elevations of erosional strandlines and cemented beach-rock ledges on the west side of the valley as minimum measures of the highstand elevation.

Highstand shorelines on the east side of the valley are extensively well-preserved, consisting exclusively of constructional beach gravel ridges developed on older alluvial fan surfaces (e.g., Fig. 4). El-

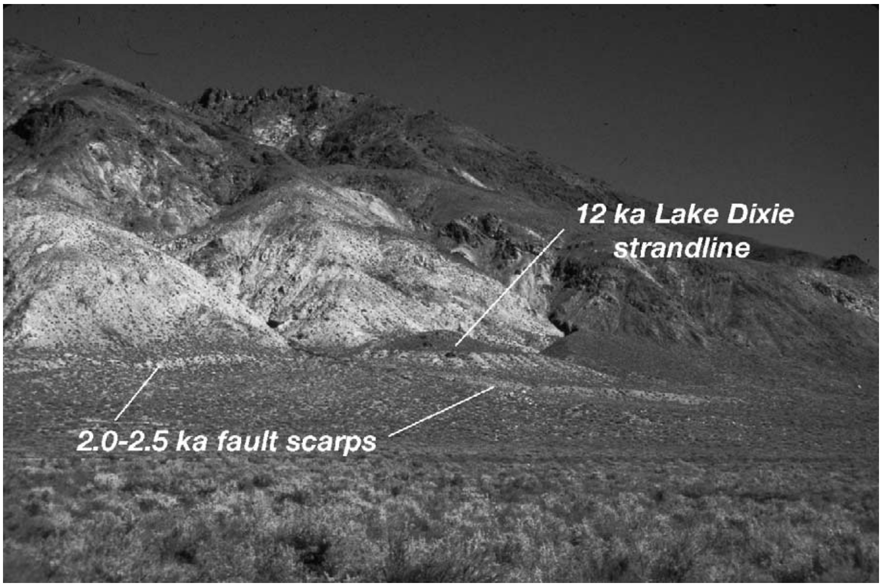

Fig. 3. Photograph toward the north of a wave-cut terrace (shoreline-angle elevation 1095.4 m) that is faulted by 2.0–2.5 ka fault rupture along the Stillwater seismic gap segment of the Dixie Valley fault (refer to Fig. 2 for location). The terrace marks the middle of three shorelines surveyed by Thompson and Burke (1973) and resurveyed during this study. The fault scarp shows 5 m of vertical separation. Fig. 6 shows a topographic profile across the terrace and fault scarp.

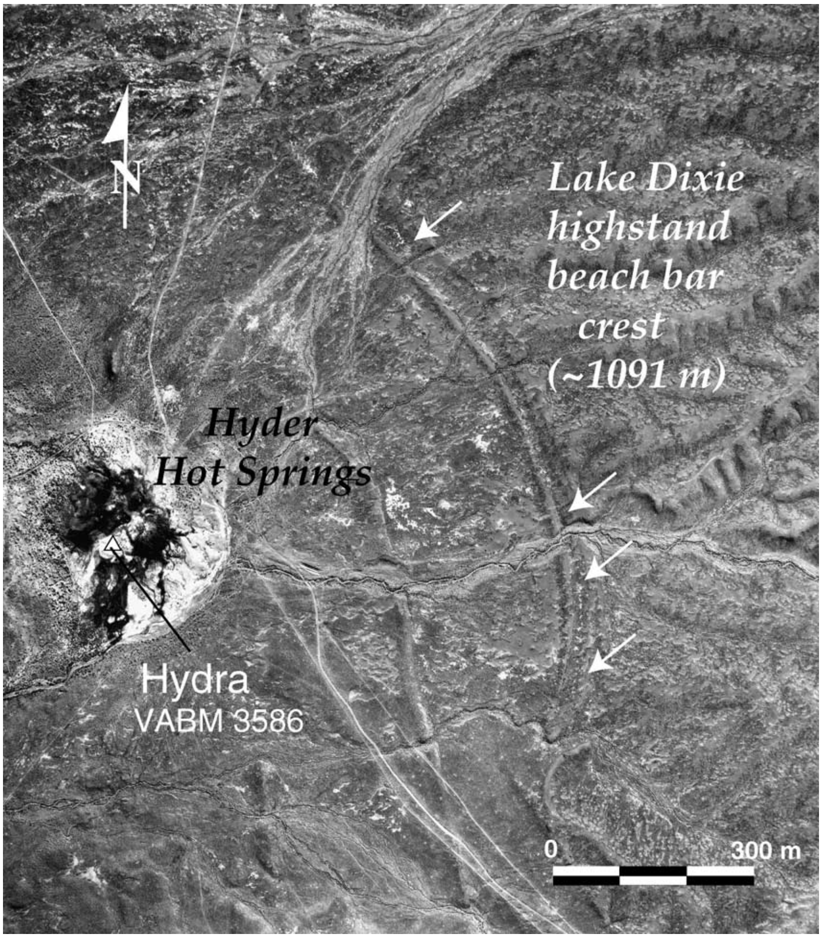

Fig. 4. 1979-vintage, low-sun-angle photograph of Lake Dixie high-stand constructional beach bar along the northeast shore (elevation 1091.4 m) (Nevada Bureau of Mines and Geology photo collection). See Fig. 2 for location. The location and approximate elevation in feet of U.S. Geodetic triangulation benchmark Hydra is shown for reference.

evations of these shorelines represent a more direct and maximum measure of the highstand. Currey (1982) indicated that crestal elevations of highstand beach ridges were largely coincident with the paleolake water plane and have a precision of ±1 m. Adams et al. (1999) reported a natural, local variation in highstand beach-ridge elevations of up to 3 m in the Lahontan basin. The smaller fetch and lower maximum wave heights expected for the smaller Lake Dixie suggest that the natural variation of beach-ridge elevations should be considerably smaller than for Lake Lahontan. Therefore, we consider elevations of the erosional shorelines and beach rock ledges on the west side of the valley as minimum estimates of the highstand, whereas we consider elevations of constructional beach ridges on the east side of the valley as a more direct estimate of the highstand, with an uncertainty of ±1 m.

3. Results

3.1. Tectonic displacement of shorelines across the Dixie Valley fault

Thompson and Burke (1973) first mapped and recognized that high-level, ∼12 ka Lake Dixie shorelines were displaced across Holocene fault ruptures along the Stillwater gap segment of the Dixie Valley fault. They surveyed shoreline elevations at three sites (Figs. 2 and 5): (1) a south site where the highest shoreline features are cemented beach rock plastered onto the uplifted footwall of the normal fault; (2) a middle site where the highest shoreline is at the back edge (i.e., shoreline angle) of a wave-cut terrace (Figs. 3 and 5) located between two strands of the fault, with the eastern strand showing Holocene vertical offsets of about 5 m and the western strand showing no obvious evidence of recent surface displacement; and (3) a north site where high-level constructional beach gravel bars lie entirely within the down-dropped hanging wall of the fault. Using a hand-level and altimeter survey (G.A. Thompson, Stanford University, personal communication) they concluded that the shorelines showed a net vertical offset of ∼9 m, with the middle site showing an elevation intermediate between the north and south sites (Fig. 6).

Recent studies of activity on the Dixie Valley fault (Caskey, 2002; Lutz et al., 2003) show that the most recent fault ruptures in the Stillwater gap formed at 2.0–2.5 ka, with a maximum vertical offset of 5 m in the shoreline survey area (e.g., Figs. 2 and 6). The 9 m of vertical offset estimated by Thompson and Burke (1973) would require at least one additional post-12 ka faulting event. However, detailed mapping along the Stillwater gap fault segment (Caskey, in preparation) has revealed no evidence for multiple Holocene fault offsets such as beveled scarps or differing vertical offsets on post-Lake Dixie fan surfaces of different ages at a given location.

We resurveyed Thompson and Burke's (1973) shoreline elevations with a total station to resolve the apparent discrepancy between mapped fault relations and the earlier survey results. We carefully identified the highest shoreline features at each of the three locations identified by Thompson and Burke (1973). Our results show that the high-level shorelines mapped by Thompson and Burke are vertically offset by only ∼5 m across the fault (Fig. 5), identical to the offsets measured across fault scarps in this area (e.g., Fig. 6). Our absolute elevations are consistently greater, and relative elevations are progressively greater from south to north compared to the previous survey elevations. We find that the elevations of the middle and south shorelines, both lying in the footwall of the recent fault breaks, are essentially identical (1095 m), indicating that no significant Holocene slip occurred along the western strand of the fault at the middle site, consistent with our field observations. Our results indicate that the hand-level/altimeter technique used by Thompson and Burke did not provide accurate results and that the previous slip rate determined from their shoreline survey is in error by about a factor of two.

3.2. Isostatic deformation of shorelines across Dixie Valley

Measurements of highstand elevations in the Lahontan Basin (Mifflin and Wheat, 1971; Adams et al., 1999) show isostatic rebound of as much as 22 m due to crustal unloading related to post-13 ka desiccation of Lake Lahontan (Fig. 1). The greatest upwarping is in the Carson Sink area where the largest volume of water existed during the last pluvial lake cycle. Lake Lahontan and Lake Dixie were coeval, so it follows that the domal rebound pattern of the Lahontan basin should be expressed by broad eastward tilting of the originally horizontal, Lake Dixie shorelines. The inferred pattern of isostatic rebound contours east of the

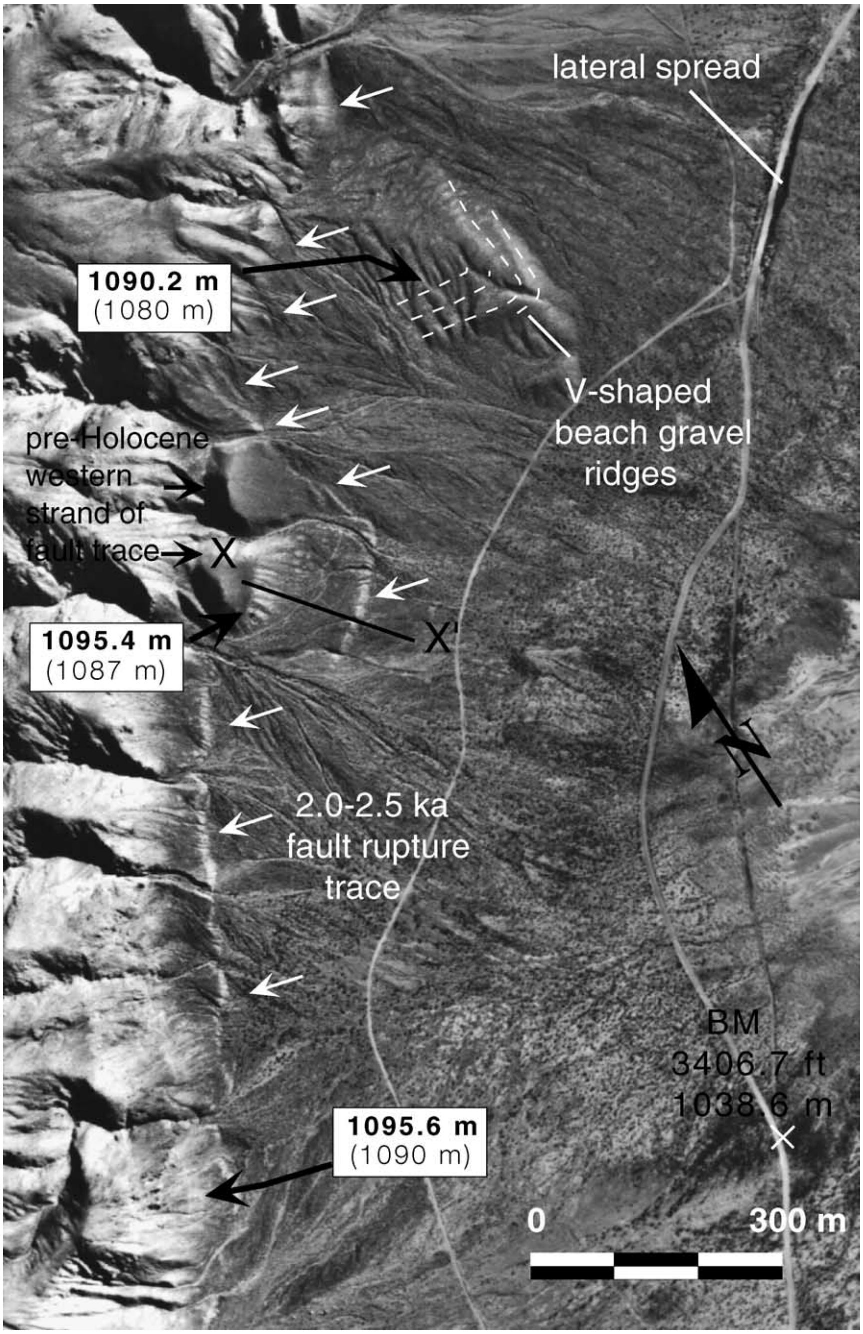
lateral spread
1090.2 m
(1080 m)
V-shaped
beach gravel
ridges
pre-Holocene
western
strand of
fault trace
X
X'
1095.4 m
(1087 m)
N
2.0-2.5 ka
fault rupture
trace
BM
3406.7 ft
1038.6 m
1095.6 m
(1090 m)
0
300 m

Fig. 5.

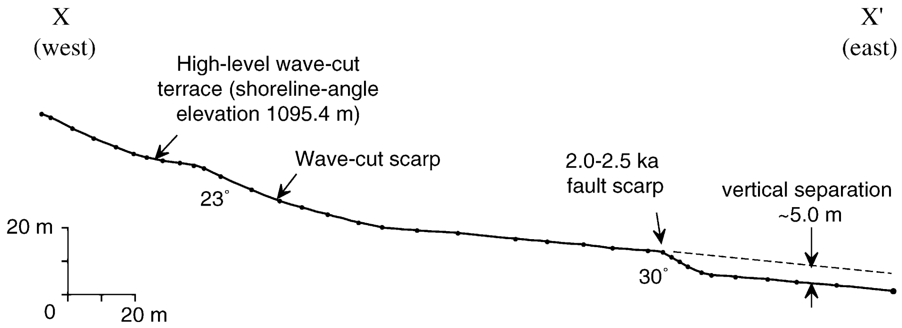

Fig. 6. Profile X–X′ of faulted wave-cut terrace (refer to Figs. 2, 3, and 5) in the area of maximum vertical offset along the 2.0–2.5 ka fault rupture trace on the Stillwater gap segment of the Dixie Valley fault. The 1095.4 m elevation is for the middle shoreline measurement shown in Fig. 5. Angles shown at the wave-cut scarp and the fault scarp are average scarp slope angles.

Lahontan basin (Fig. 1, Adams et al., 1999) suggests that we might expect to see ≥6 m of eastward tilting across Dixie Valley. To test this hypothesis and potentially provide an extended lithospheric deflection datum, we collected elevation measurements at 16 sites along the Lake Dixie highstand shoreline (Fig. 2).

The Lake Dixie shoreline elevation data are projected onto an east–west profile (Fig. 7). Error bars of ±1 m were assigned to the constructional beach bars measured on the east side of the valley (between the 16- and 44-km marks) based on the criteria previously discussed. The scatter observed in this part of the data set probably results from natural variability in the original beach bar crest elevations. The scatter in the elevations to the west probably results from natural variation and other factors. For example, the three elevations at the 11-km mark (Fig. 7) are from both high-level strandlines and beach rock deposits, which do not necessarily mark the highest level reached by the lake. The two westernmost elevation measurements are from remnants of shoreline deposits that are elsewhere buried by younger Holocene alluvial fan deposits, so we do not know if these are actually highstand deposits. Additionally, all of the shoreline features surveyed on the west side of the valley are very close to Holocene fault scarps, with the southwesternmost sites also lying adjacent to 1954 Dixie Valley fault ruptures. Therefore, differential tectonic uplift (at footwall sites) and subsidence (at hanging wall sites) have undoubtedly affected their present day elevations (see Section 4 below).

The distribution of high shoreline elevations shows convincingly that Lake Dixie shorelines are tilted to the east (Fig. 7). Linear regression of the entire elevation data set shows an eastward tilt of 0.13 m/km (Fig. 7). A data subset that includes only the beach bar crest elevations along the east side of the valley indicates an eastward tilt of 0.16 m/km (Fig. 7). The two highest strandline elevations on the west side of the valley combined with the beach bar crest elevations on the east side indicate an eastward tilt of 0.20 m/km (Fig. 7). We interpret the beach bar crests on the east side of the valley to provide the most reliable measure of tilt (i.e., 0.16 m/km) because these are consistent shoreline types, they are the type

---

Fig. 5. 1979-vintage, low-sun-angle photograph of the survey area of high-level shorelines displaced by the 2.0–2.5 ka fault ruptures along the Stillwater seismic gap segment of the Dixie Valley fault (Nevada Bureau of Mines and Geology photo collection). Boxes show shoreline elevations determined in this study (bold) and previously estimated shoreline elevations (not bold) (Thompson and Burke, 1973). Elevations in this study were measured relative to the 3406.7 ft (1038.6 m) U.S. Geodetic Survey benchmark shown and adjusted to the 1988 North American vertical datum (NAVD 88). White arrows mark the 2.0–2.5 ka fault rupture trace. Refer to text for discussion.

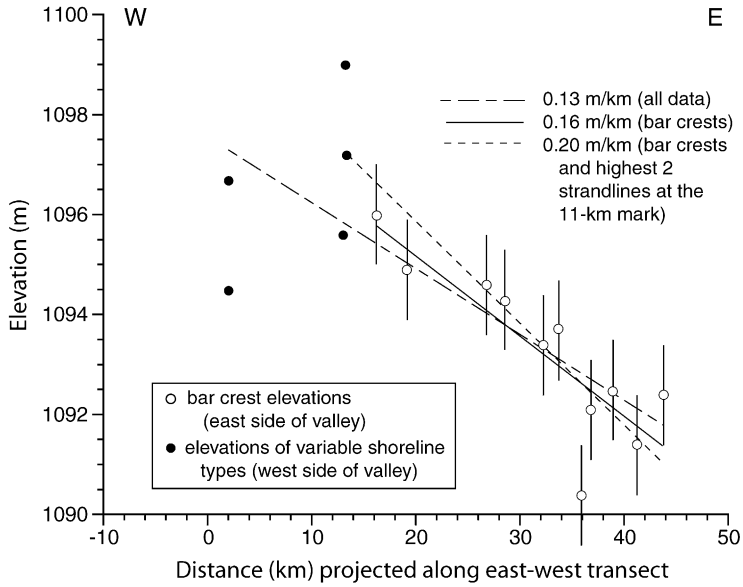

Fig. 7. Lake Dixie high-shoreline elevations projected orthogonally onto the east–west-trending part of profile A–A′ (Figs. 1 and 2) and illustrating eastward tilt across the valley. Linear regression lines are defined with their slope values for three data subsets. We consider the east-tilt of the bar crest elevations along the east side of the valley to be the best constrained measure of tilt because bar crest elevations provide the most reliable measure of the lake high stand and because these sites are unlikely to be strongly affected by Holocene and historic vertical fault movements along the Dixie Valley fault on the west side of the valley. The 0-km mark (*x*-axis) coincides with the bend in profile line A–A′ located along the west side of Dixie Valley.

of shoreline feature that best represents the highstand, and they are farthest removed from deformation associated with Holocene and historic faulting along the west side of the valley. The set of bar crest elevation data contains one statistical outlier at the 36-km mark (elevation 1090.4 m, Fig. 7). Aerial photographs suggest the presence of a subtle, higher shoreline at this location (Fig. 2), but we were

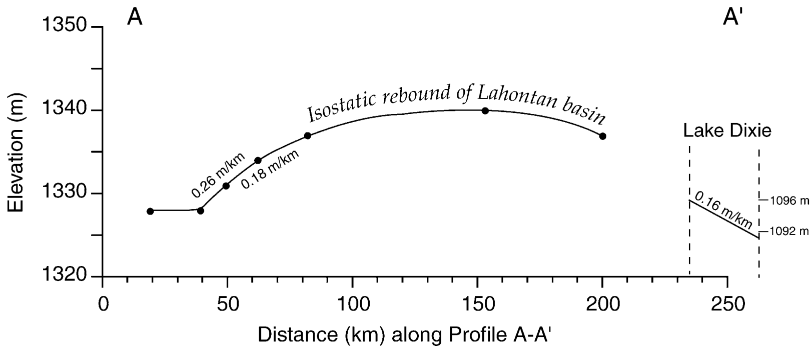

Fig. 8. Isostatic rebound profile A–A′ (see Fig. 1 for profile location). Dixie Valley shorelines formed at a different elevation than those in the Lahontan basin, so a separate elevation scale is shown to the right of the Dixie Valley flexure datum. The solid line representing east-tilt and isostatic flexure across Dixie Valley is from the linear regression line through the bar crest elevation data (Fig. 7) from the east shore of Lake Dixie. See text for discussion.

unable to definitively locate the higher shoreline in the field. If we exclude the 1090.4 m elevation, then the estimated eastward tilt from the bar crest elevations is 0.15 m/km.

By combining the isostatic rebound data from the Lake Lahontan basin (Adams et al., 1999) with the Lake Dixie shoreline data we extend a northwest–southeast rebound profile to the east to more fully characterize lithospheric deflection resulting from isostatic rebound of the Lahontan basin (Fig. 8). For simplicity, we pick values from the shoreline elevation contours in the western and central parts of the Lahontan basin (Adams et al., 1999). Lake Dixie was at a lower elevation than Lake Lahontan, so the elevation scale for Lake Dixie is shifted upward by about 330 m. The eastward tilt of bar crest elevations on the east side of Dixie Valley (0.16 m/km) indicates lithospheric deflection that is essentially symmetrical with deflection on the west side of the Lahontan basin.

4. Discussion

4.1. Possible influence of tectonic deformation on the record of eastward tilting

Using the paleoshoreline data in Dixie Valley as a tiltmeter is complicated by the Holocene and historic movements along the Dixie Valley normal fault (Fig. 2). The 1954 M_s 6.8 Dixie Valley earthquake produced surface ruptures along a 45-km section of the fault with vertical offsets of up to 2.8 m (Caskey et al., 1996). Most of this rupture zone is shown in Fig. 2. A late Holocene earthquake dated at 2.0–2.5 ka also produced a 45-km-long zone of surface ruptures, which extend along the southern part of the Stillwater seismic gap and overlap with the 1954 ruptures to the south by about 22 km (Bell and Katzer, 1990; Caskey, 2002; Lutz et al., 2003). The late Holocene ruptures exhibit very localized maximum vertical offsets of about 5 m (Figs. 2 and 6) although most vertical offsets along this rupture zone range from 1.5 to 2.5 m. Holocene fault ruptures of uncertain age have also been mapped along the fault in northernmost Dixie Valley, where scarps exhibit vertical offsets of 1.0–1.5 m (Smith, 2000; Caskey, in preparation). No Holocene fault ruptures have been recognized on the east side of Dixie Valley (Dohrenwend et al., 1996). A distribution of representative net vertical offset measurements (i.e., Holocene plus historic offsets, where appropriate) is shown along the Dixie Valley fault in Fig. 2.

To evaluate the possible effects of fault displacements on the eastward tilt signal, we use the results of geodetic leveling across the 1983 Borah Peak, Idaho earthquake rupture on the Lost River fault as an analogue (Fig. 9; Stein and Barrientos, 1985; Barrientos et al., 1987). The Lost River fault appears to be an appropriate analogue for comparing coseismic displacements across the Dixie Valley fault because: (1) both are Basin and Range normal faults; (2) both have similar dips (49–52°) and exhibit planar subsurface geometry. These factors are at least true for the Stillwater gap segment of the Dixie Valley fault based on extensive borings in the Dixie Valley geothermal field (Benoit, 1995); the central part of the segment that ruptured in the 1954 event locally exhibits a shallower dip of 25–30° (Caskey et al., 1996; Abbott et al., 2001), although this part of the fault overlaps with only the southern end of Lake Dixie; and (3) the amount of vertical displacement across the Borah Peak earthquake rupture (∼2.0 m) is similar to net vertical offsets measured along most the Dixie Valley fault (1.5–3.0 m). Our preferred measure of eastward tilting across Dixie Valley is based on shoreline features on the east side of the valley, so we are primarily concerned with far-field, tectonically induced elevation changes at distances of 12–18 km from the fault. Fig. 9b shows absolute elevation changes across the Borah Peak fault rupture along leveling route A–A′ (Fig. 9a), which indicates that points in the hanging wall at distances of 12–18 km from the fault

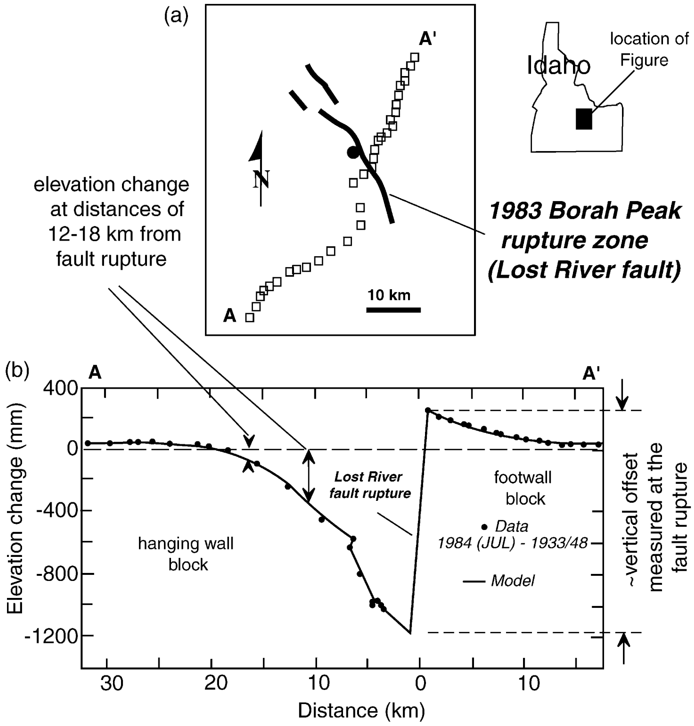

Fig. 9. Geodetic survey line (a) and elevation change profile (black dots) and coseismic dislocation model (b) across the 1983 Borah Peak earthquake rupture zone on the Lost River (normal) fault, Idaho (Stein and Barrientos, 1985; Barrientos et al., 1987). Square symbols in (a) are benchmarks surveyed in 1933/1948 and 1984. The elevation change profile provides an analogue for expected coseismic elevation changes on the east side of Dixie Valley due to Holocene and historic fault offset along the Dixie Valley fault on the western side of the valley. See text for discussion.

surface rupture show little absolute elevation change. At a distance of 12 km from the surface rupture, the absolute elevation decrease is approximately 20% of the total vertical offset measured at the fault scarp. Because most of the net vertical offsets along the fault range from 1.5 to 3.0 m, this equates to absolute elevation decreases of 0.3–0.6 m, which is significantly less than the uncertainty we place on beach bar crest elevations due to natural variation. At a distance of 18 km from the surface rupture, the absolute elevation decrease is only about 10% of the vertical offset measured at the fault scarp. We suggest that elevation changes across the 1983 Borah Peak earthquake rupture zone are an appropriate analogue for tectonic deformation in Dixie Valley and that Holocene tectonic deformation along the Dixie Valley fault does not significantly affect the signal of eastward tilting recorded by beach bar crest elevations along the east shore of Lake Dixie.

4.2. Implications of new survey data for slip rates on the Dixie Valley fault

The results of our resurvey of faulted shorelines in the Stillwater gap area indicate that the high-level shorelines identified by Thompson and Burke (1973) are offset by only 5 m, rather than the 9 m offset estimated from less precise survey techniques. It should be noted that a potential pitfall in using these particular shoreline features as displacement markers lies in the observation that each of the three features are of a different type (i.e., cemented beach rock ledge, shoreline angle of a wave-cut terrace, and beach gravel deposits), and it is uncertain whether all three features formed at the same lake level. Nevertheless, the 5 m of apparent vertical offset is identical to the maximum vertical offset measured across scarps in the survey area. More importantly, the smaller apparent vertical offset, together with detailed mapping and paleoseismic studies along the fault, show that the shorelines in this area have been deformed by a single surface-rupturing earthquake dated at 2.0–2.5 ka. These observations preclude using the faulted shorelines to accurately estimate fault slip rate because they have not yet experienced a complete earthquake cycle. Therefore, we consider invalid the often-cited Dixie Valley extension rate of 1 mm/a (Thompson and Burke, 1973), which was based on the earlier shoreline survey and additional indirect reasoning.

Holocene slip rates for the Dixie Valley fault are better constrained to the south in The Bend area (Fig. 2) where the fault has experienced both a Holocene and a historic surface rupture. In The Bend area, Bell and Katzer (1990) and Caskey et al. (1996) measured net Holocene vertical offsets of 4–6 m across a complex zone of faults yielding a vertical slip rate of 0.3–0.5 mm/a since the 12 ka lake stand. We consider this rate a maximum because it is based on less than two complete earthquake cycles on the fault. Approximately 30 km south of The Bend, the north end of the Sand Springs segment of the Dixie Valley fault has experienced three post ∼13 ka paleoseismic events with a total vertical offset of 6 m, similarly indicating a maximum vertical slip rate of ∼0.5 mm/a (Bell et al., in press). These Holocene slip rates are similar to long-term vertical slip rate estimates for the Stillwater Range of 0.3–0.4 mm/a based on vertically displaced Miocene volcanic rocks (Wallace and Whitney, 1984; Okaya and Thompson, 1985).

5. Conclusions

New elevation data from late Pleistocene (∼12 ka) pluvial Lake Dixie shorelines reveal that these features record far-field lithostatic flexure due to isostatic rebound of the Lake Lahontan basin. Linear regression analysis of beach bar crest elevations on the east side of Dixie Valley indicate eastward tilt with a slope gradient of 0.16 m/km. Shorelines on the west side of the valley are disrupted by both historic and late Holocene surface ruptures on the Dixie Valley normal fault, so it is possible that the tilt signal of the east side shorelines is complicated by fault displacements. However, detailed geodetic data across the 1983 Borah Peak, Idaho earthquake rupture (Lost River fault) show that coseismic elevation changes decrease rapidly with distance from normal fault ruptures and at distances of >10 km equate to only a small percent of the vertical offset measured at the fault. The Lost River fault ruptures appear to be an appropriate analogue for those in Dixie Valley since both faults have similar geometry and the amount of vertical fault offsets being considered is similar for the two areas. We therefore suggest that Holocene fault displacements do not significantly affect the eastward tilt recorded along the east shore of Lake Dixie.

The Lake Dixie shoreline data combined with the isostatic rebound data from the Lahontan basin defines eastward tilting and lithospheric deflection to be essentially symmetrical with deflection along the west side of the Lahontan basin. The symmetry of the deflection suggests that previous estimates of upper mantle viscosity beneath the Lahontan basin (10^{18} Pa s; Bills et al., 1995) may be applicable to a broader region extending at least as far east as Dixie Valley.

Faulted shorelines on the west side of Dixie Valley exhibit about 5 m of vertical displacement across a single, late Holocene fault rupture, in contrast to the results of a previous survey that suggested ∼9 m of vertical offset inferably across multiple Holocene surface ruptures (Thompson and Burke, 1973). The new survey data refutes the 1 mm/a Holocene extension rate across Dixie Valley estimated from the earlier survey. Holocene vertical slip rates of 0.3–0.5 mm/a have been estimated elsewhere along sections of the fault that have experienced multiple Holocene surface fault ruptures.

Acknowledgements

This study was supported in part by U.S. Department of Energy Grant DE-FG07-98ID113620. The views and conclusions contained in this document are those of the authors and should not be interpreted as necessarily representing the official policies, either expressed or implied, of the U.S. Government. This study would not have been possible without the field assistance of Rick Ford, Gary Schneider, Michael W. Goebel, Nathan W. Smith, Carolyn Domrose, Tandis S. Bidgoli, and Anne Marie Scherer. Ken Adams and participants of the 2002 Pacific Cell Friends of the Pleistocene Field Trip provided helpful insights and discussions. The manuscript also benefited from a review by Keith Benn.

References

Abbott, R.E., Louie, J.N., Caskey, S.J., Pullammanappalli, S., 2001. Geophysical confirmation of low-angle normal slip on the historically active Dixie Valley fault, Nevada. J. Geophys. Res. 106 (B3), 4169–4181.

Adams, K.D., Wesnousky, S.G., 1998. Shoreline processes and the age of the Lake Lahontan highstand in the Jessup embayment. Geol. Soc. Am. Bull. 110 (6), 1318–1332.

Adams, K.D., Wesnousky, S.G., Bills, B.G., 1999. Isostatic rebound, active faulting, and potential geomorphic effects in the Lake Lahontan basin, Nevada and California. Geol. Soc. Am. Bull. 111 (12), 1739–1756.

Barrientos, S.E., Stein, R.S., Ward, S.N., 1987. Comparison of the 1959 Hebgen Lake, Montana and the 1983 Borah Peak, Idaho, earthquakes from geodetic observations. Bull. Seism. Soc. Am. 77 (3), 784–808.

Bell, J.W., Katzer, T., 1990. Timing of late Quaternary faulting in the 1954 Dixie Valley earthquake area, central Nevada. Geology 18, 622–625.

Bell, J.W., Caskey, S.J., Ramelli, A.R., Guerrieri, L., in press. Pattern and rates of faulting in the 1954 portion of the central Nevada seismic belt and paleoseismic evidence for older belt-like behavior. Bull. Seism. Soc. Am.

Benoit, D., 1995. Force folding and Basin and Range geothermal systems. Geotherm. Resour. Council Trans. 19, 155–163.

Benson, L.V., Thompson, R.A., 1987. Lake-level variation in the Lahontan basin for the past 50,000 years. Quaternary Res. 28, 69–85.

Bills, B.G., May, G.M., 1987. Lake Bonneville: constraints on lithospheric thickness and upper-mantle viscosity from isostatic warping of Bonneville, Provo, and Gilbert stage shorelines. J. Geophys. Res. 92, 11493–11508.

Bills, B.G., Adams, K.D., Wesnousky, S.G., 1995. Estimates of upper mantle viscosity in the western Great Basin from Lake Lahontan shoreline elevation patterns. Eos (Trans., Am. Geophys. Union) 76, F608.

Broecker, W.S., Kaufman, A., 1965. Radiocarbon chronology of Lake Lahontan and Lake Bonneville II, Great Basin. Geol. Soc. Am. Bull. 76, 537–566.

Brotchie, J.F., Silvester, R., 1969. On crustal flexure. J. Geophys. Res. 74, 5240–5252.

Caskey, S.J., Wesnousky, S.G., Zhang, P., Slemmons, D.B., 1996. Surface faulting of the 1954 Fairview Peak (M_s 7.2) and Dixie Valley (M_s 6.8) earthquakes, central Nevada. Bull. Seism. Soc. Am. 86, 761–787.

Caskey, S.J., 2002. Age of faulting in the Stillwater gap and lateral-spread-induced contraction along the playa margin. In: Caskey, S.J. (Ed.), Historical Faulting, Chronostratigraphy, and Paleoseismicity of the Central Nevada Seismic Belt, 2002 Pacific Cell Friends of the Pleistocene Field Trip Guide, pp. 109–114.

Crittenden, M.D., 1963. New data on the isostatic deformation of Lake Bonneville. U.S. Geol. Surv. Prof. Pap. 454, E1–E31.

Currey, D.R., 1982. Lake Bonneville: selected features of relevance to neotectonic analysis. U.S. Geol. Surv. Open-File Rep. 31, 82–1070.

Dohrenwend, J.C., Schell, B.A., Menges, C.M., Moring, B.C., McKittrick, M.A., 1996. Reconnaissance photogeologic map of young (Quaternary and late Tertiary) faults in Nevada. Nevada Bureau of Mines and Geology, Open File Report, OFR 96-2, in Cooperation with the U.S. Geologic Survey, Scale 1:1,000,000.

Gilbert, G.K., 1890. Lake Bonneville. US Geol. Surv. Monograph 1.

Lutz, S.J., Caskey, S.J., Johnson, S.D., 2003. Geyserite, faulted sinter terraces, and other fossil hot spring deposits, northern Dixie Valley fault system, Nevada. In: Foster, S. (Ed.), Nevada Petroleum Society 2003 Field Trip Guidebook, pp. 75–89.

May, G.M., Bills, B.G., Hodge, D.S., 1991. Far-field flexural response of Lake Bonneville from paleopluvial lake elevations. Phys. Earth Planet. Interiors 68, 274–284.

Mifflin, M.D., Wheat, M.M., 1971. Isostatic rebound in the Lahontan basin, northwestern Great Basin. Geol. Soc. Am. Abstracts Programs 3, 647.

Mifflin, M.D., Wheat, M.M., 1979. Pluvial lakes and estimated pluvial climates of Nevada. Nevada Bureau Mines Geol. Bull. 94, 57.

Nakiboglu, S.M., Lambeck, K., 1982. A study of the earth responses to surface loading with application to Lake Bonneville. Geophys. J. R. Astron. Soc. 70, 577–620.

Okaya, D.A., Thompson, G.A., 1985. Geometry of Cenozoic extensional faulting: Dixie Valley, Nevada. Tectonics 4, 107–125.

Passey, Q.P., 1981. Upper mantle viscosity derived from the difference in rebound of the Provo and Bonneville shorelines, Lake Bonneville basin. J. Geophys. Res. 86, 11701–11708.

Reheis, M., 1999. Extent of Pleistocene lakes in the western Great Basin: U.S. Geol. Surv. Misc. Field Studies Map MF 2323 (online version, http://geo-nsdi.er.usgs.gov/metadata/map-mf/2323/metadata.faq.html).

Smith, N.W., 2000. Paleoseismic Activity of the Stillwater Gap Segment of the Dixie Valley Fault: Evidence from the Tectonic Geomorphology of Alluvial Fans near the Sou Hills, Central Nevada. B.S. Thesis, San Francisco State University, San Francisco, CA, p. 18.

Stein, R.S., Barrientos, S.E., 1985. Planar high-angle faulting in the Basin and Range: geodetic analysis of the 1983 Borah Peak, Idaho earthquake. J. Geophys. Res. 90, 355–366.

Thompson, G.A., Burke, D.B., 1973. Rate and direction of spreading in Dixie Valley, Basin and Range province. Nevada Geol. Soc. Am. Bull. 84, 627–632.

Walcott, R.I., 1970. Flexural rigidity, thickness and viscosity of the lithosphere. J. Geophys. Res. 75, 3941–3954.

Wallace, R.E., Whitney, R.A., 1984. Late Quaternary history of the Stillwater seismic gap, Nevada. Bull. Seism. Soc. Am. 74 (1), 301–314.